TIDALLY DRIVEN FAULT DEFORMATION AND STRESS ACCUMULATION AT ENCELADUS'S TIGER STRIPES. Bridget R. Smith-Konter[1] (Bridget.R.Konter@jpl.nasa.gov), Zane Crawford[1,2], and Robert T. Pappalardo[1], [1]Jet Propulsion Laboratory, California Institute of Technology, [2]Laboratory for Atmospheric and Space Physics, University of Colorado, Boulder.

Introduction: Cassini observations of the south polar region of Enceladus revealed four large linear fractures associated with anomalous temperature gradients and active plumes [1, 2]. These features, referred to as "tiger stripes", are now thought to be the source of tectonic strike-slip and/or oblique open-close motions [3,4], similar to those of the faulting regimes inferred for Jupiter's moon Europa [5]. These motions are likely a result of tidally induced stresses that are exerted on a satellite during its daily orbital (diurnal) cycle around its parent body.

In this study, we investigate tidally driven strike-slip and fault-normal deformation of Enceladus's tiger stripes and their resulting failure stress behavior over a complete Enceladus tidal cycle. We simulate 3D surface deformation and stress changes at depth by specifying tidally induced stresses across inferred tiger stripe fault planes. Our approach can be summarized in three primary steps: (1) calculate tidal stresses that will act as the driving forces for shearing and normal motions; (2) integrate these stresses into a 3D time-dependent fault dislocation model to evaluate tidally induced displacements and stress changes at depth; (3) calculate resulting fault-to-fault stress interactions and failure conditions as a function of position within the orbital cycle.

While previous studies have followed a similar approach to investigate individual modes of failure (shear vs. normal) of the tiger stripes [3, 4], this work differs in that (1) contributions of both shear and normal stress are considered and (2) a sophisticated 3D viscoelastic dislocation model is used to kinematically drive displacements and inspect resulting stress changes of the tiger stripe fault system. Here we present preliminary results demonstrating the role of aseismic secular displacements at depth, which impart stress changes onto each tiger stripe fault plane within the shallow brittle layer. As an example of this method, we demonstrate this behavior for tidally induced left-lateral strike-slip motions for the first half of Enceladus's orbit. Future applications of this approach are valid for deformation studies of Europa and other icy moons of the outer solar system where diurnal stress variations are important.

Stress Modeling:

Tidal Stress Model. We assume that diurnal tidal stresses provide sufficient driving forces for shear and normal fault motions to occur along the tiger stripe fractures. To extract the tidal diurnal stress components, we utilize the computer program SatStress [6], a numerical modeling code that calculates the 2D tidal stress tensor at any point on the surface of an icy satellite for diurnal and/or non-synchronous rotation stresses. We adopt model parameters appropriate for an Enceladean ice shell of thickness 24 km underlain by a global subsurface ocean [3]: Love numbers h_2 = 0.2 and l_2 = 0.04, shear modulus μ = 3.5 GPa, Poisson ratio ν = 0.33, gravity g = 0.11 m/s^2, radius r = 252 km, and eccentricity e = 0.0047. For Enceladus, we also assume that satellite obliquity is zero and we neglect any non-synchronous rotation. Using these parameters, we calculate tidal diurnal stresses in the region of the tiger stripe fractures, which approach peak absolute amplitudes of ~70 kPa throughout the tidal cycle. To provide shear and normal driving stresses for the dislocation model, we resolve shear (τ_s) and normal (σ_n) stresses onto discrete tiger stripe fault elements of specified orientation [3, 4, 7].

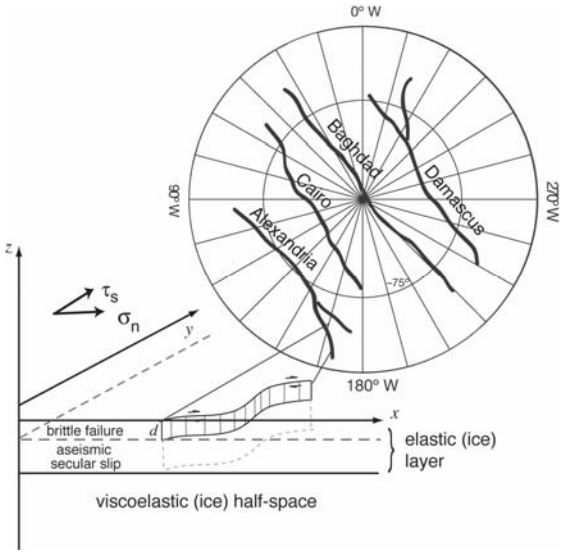

Fig 1. Polar stereographic projection of Enceladus tiger stripes and 3D sketch of viscoelastic dislocation model. Deformation is kinematically driven by prescribed diurnal tidal stresses at each tiger stripe location throughout the tidal cycle. Discrete vertical fault planes are embedded in an elastic ice layer that responds to both shallow brittle failure and deep secular slip. Both near-field (shallow, coseismic) and far-field (deep, aseismic) displacements can be prescribed along each fault plane.

Viscoelastic Dislocation Model. Using the tidal stresses derived above, we simulate strike-slip (shear) and open-close (normal) surface deformation on a set vertical fault planes embedded in an elastic layer overlying a viscoelastic half-space (Fig. 1). We use a 3D semi-analytic dislocation model [8, 9], originally developed for terrestrial applications, which calculates displacement, stress, and strain caused by horizontal shear, vertical shear, or fault-normal displacement as a

function of depth. The model assesses displacements and stresses at variable temporal scales. Analogous to a fractured terrestrial tectonic plate, shallow brittle failure drives both an elastic and time-dependent viscoelastic response at depth due to a redistribution of stress imparted by the breaking of a fault. Secular (or long-term, time-invariant) slip beneath the fault assumes a purely elastic model and captures the aseismic response of the moving fault system. The model is sensitive to fault locking (or brittle-layer thickness) depth d, total elastic ice layer thickness (which includes zones of both aseismic and brittle failure), viscosity η, and the restoring force of gravity, g. Here we assume d = 4 km, $\eta = 10^{15}$ Pa s, and other model parameters identical to those used to derive the tidal stresses.

The tiger stripe dislocations are projected about an effective pole of deformation and placed into a model-space Cartesian coordinate system (Fig. 2). We apply a depth-integrated stress [10] that drives slip at depth, which then generates stress changes within the shallow brittle (locked) layer. Both shear and normal stresses are applied along the vertical fault patches as a function of orbital position. The applied shear stresses mainly drive fault-parallel strike-slip displacements, while normal stresses control the opening and closing displacements of the fracture system.

To investigate the role of stress change within the brittle layer as a function of orbital position, we also calculate Coulomb stress change, σ_f [7]. According to the Coulomb failure criterion ($\sigma_f = \tau_s - \mu_f \sigma_n$), frictional sliding will occur on optimally oriented fault segments when the resolved shear stress exceeds the frictional resistance on the fault, which is a function of the normal stress and the effective coefficient of friction (μ_f = 0.3-0.7). We compute Coulomb stress change to identify regions of the fault system that are more or less likely to fail throughout the tidal cycle for a given set of applied conditions. We also use Coulomb calculations to investigate the implications of stress triggering (enhanced failure conditions on a fault segment due to an imparted coseismic stress change on neighboring fault segments), and any temporal variations in stress due to viscoelastic relaxation.

Preliminary Results: Using tidally driven stresses, which are resolved onto the tiger stripe fault planes as a function of orbital cycle, we simulate shear aseismic displacements and generate maximum shear deformation at periapse (left-lateral) and apoapse (right-lateral). These deformations range from +/- 20 mm in the horizontal (fault parallel and perpendicular) directions and +/- 2 mm of vertical uplift and subsidence. Likewise, maximum Coulomb stress change for the entire fault system (Fig. 2) is inferred at periapse (left-lateral shear) and weakens as Enceladus advances in orbital location, reaching a minimum at periapse + 120°. Subsequent orbital positions yield an increased Coulomb stress change, although in a right-lateral sense, as the satellite approaches apoapse. This behavior is repeated, although in the opposite sense, as the second half of the orbital cycle is completed. Using the Coulomb failure criterion, it is feasible to predict failure direction, frequency, and location along each tiger stripe throughout the orbital cycle. We are presently compiling a suite of time-dependent models that simulate these stress behaviors, in addition to those of tidally forced dislocations due to the opening/closing of a fault, to investigate possible failure scenarios and stress triggering interactions of the tiger stripe fault system.

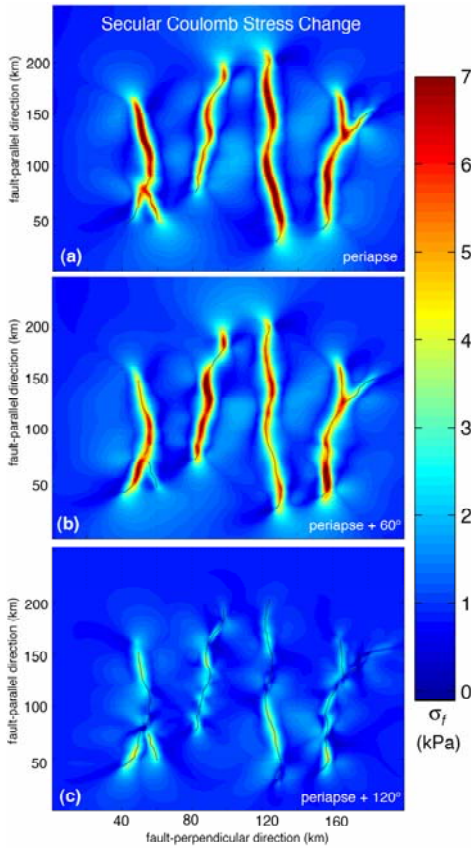

Fig. 2. Snapshots of secular Coulomb stress change, σ_f (kPa), due to tidally induced left-lateral displacements within the deep aseismic layer, observed at (a) periapse, (b) periapse + 60°, and (c) periapse + 120°. Stresses are observed at a depth of 2 km within the brittle layer. Large, positive stresses are indicative of fault segments that are brought closer to failure within the brittle layer.

References: [1] Porco, C.C. et al. (2006), *Science*, 311, 1393-1401. [2] Spencer, J.R. et al. (2006), *Science*, 311, 1401-1405. [3] Nimmo, F. et al. (2007), *Nature*, 447, 289-291. [4] Hurford, T.A. et al. (2007), *Nature*, 447, 292-294. [5] Hoppa, G.V. et al. (1999), *Icarus*, 141, 287-298. [6] Wahr, J. et al., in preparation. [7] King.G.C.P. et al. (1994) *BSSA*, 84, 935-953. [8] Smith, B., and D.T. Sandwell (2003), *JGR.*, 108, doi:10.1029/2002JB002136. [9] Smith, B., and D.T. Sandwell (2004), *JGR*, doi:10.1029/2004JB003185. [10] Sandwell D.T. et al. (2004), *JGR*, 109, doi:10.1029/2004JE002276.